Separation Science and Technology
Publication details, including instructions for authors and subscription information:
http://www.informaworld.com/smpp/title~content=t713708471

Recovery of Deuterium from Water-Isotopes Mixture in Flat-Plate Thermal-Diffusion Columns of the FRAZIER Scheme with Optimal Plate Aspect Ratio for Improved Performance

Ho-Ming Yeh[a]
[a] Department of Chemical and Materials Engineering, Tamkang University, Tamsui, Taiwan

To cite this Article Yeh, Ho-Ming(2007) 'Recovery of Deuterium from Water-Isotopes Mixture in Flat-Plate Thermal-Diffusion Columns of the FRAZIER Scheme with Optimal Plate Aspect Ratio for Improved Performance', Separation Science and Technology, 42: 12, 2629 — 2643
To link to this Article: DOI: 10.1080/01496390701515094
URL: http://dx.doi.org/10.1080/01496390701515094

Separation Science and Technology, 42: 2629–2643, 2007

ISSN 0149-6395 print/1520-5754 online
DOI: 10.1080/01496390701515094

Recovery of Deuterium from Water-Isotopes Mixture in Flat-Plate Thermal-Diffusion Columns of the FRAZIER Scheme with Optimal Plate Aspect Ratio for Improved Performance

Ho-Ming Yeh
Department of Chemical and Materials Engineering, Tamkang University, Tamsui, Taiwan

Abstract: The equations for estimating the optimal plate aspect ratio as well as the corresponding maximum recovery, maximum production rate, and minimum plate surface area for recovery of deuterium from water-isotopes mixture in flat-plate thermal diffusion columns of the Frazier scheme, have been derived. Considerable improvement in performance is obtainable if the operation is carried out with the optimal plate aspect ratio. It was found that all the optimal plate aspect ratios, as well as the improvements in performance, do not depend on feed concentration.

Keywords: Thermal diffusion, deuterium, plate aspect ratio, Frazier scheme

INTRODUCTION

With deuterium as the resource, fusion energy may be the coming nuclear energy, instead of fission energy, in the distance future. The separation of hydrogen isotope in large cryogenic distillation columns has been effectively investigating in the Los Alamos National Laboratory. The hydrogen isotope inventory in a cryogenic distillation column was estimated numerically, and the results were confirmed experimentally (1). The fraction of hydrogen

Received 6 February 2007, Accepted 17 April 2007
Address correspondence to Ho-Ming Yeh, Department of Chemical and Materials Engineering, Tamkang University, Tamsui, Taipei County 251, Taiwan. Fax: (886) 226-209887; E-mail: hmyeh@mail.tku.edu.tw

isotopes in crystal water of crystalline hydrates was also investigated and discussed (2). Thermal diffusion is a well-established method for separating isotopes (3, 4). For separation of hydrogen isotopes, this process is particularly attractive because of the large ratio in molecular weights (5). Enrichment of heavy water from water-isotopes mixture by thermal diffusion in a Clusius-Deckel column was studied both theoretically and experimentally in the previous work (6). Recently, the isotopic water separation using an air gap membrane distillation (AGMD) and vacuum enhanced membrane distillation (VEMD) was also successfully investigated (7). In industrial applications, thermal diffusion columns are connected in series such as that shown in Fig. 1, called the Frazier scheme (8). An analytical solution for the separation theory in the Frazier scheme was given by Rabinovich and Sovorov (9, 10).

The flat-plat thermal diffusion column consists essentially of two opposing parallel plates separated by a very narrow open space. One plate is heated and the other cooled, and the thermal diffusion effect produced by the temperature gradient causes one component, say component 1, to diffuse toward the cold plate. At the same time, the density gradient that arises because of the temperature gradient causes smooth laminar convection currents to move up the hot plate and down the cold plate. Because of the concentration gradient set up by thermal diffusion, the convective currents transport component 1 preferentially toward the bottom and thus create substantial concentration differences between the top and bottom of the column. The convective currents in a thermal-diffusion column actually have two conflict effects: the desirable cascading effect and the undesirable remixing effect (11, 12). Therefore, proper control of the convective strength might effectively suppress this undesirable remixing effect while still preserving the desirable cascading effect, thereby leading to improved separation.

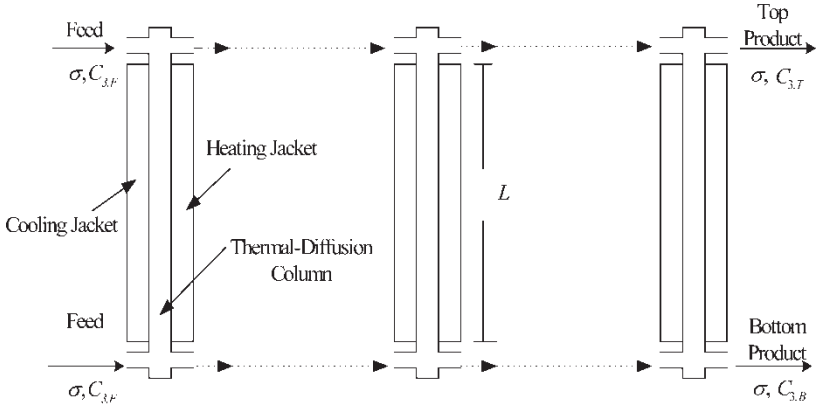

Figure 1. Schematic diagram of the Frazier scheme with N flat-plate thermal diffusion columns connected in series.

One of the effective ways for the improvement of separation by properly controlling the convective strength in flat-plate thermal-diffusion columns is suitably adjusting the plate aspect ratio (13). It is the purpose of the present study to investigate the effect of plate aspect ratio on the recovery of deuterium from water-isotopes mixture in flat-plate thermal-diffusion columns of the Frazier scheme.

SEPARATION THEORY

Degrees of Separation for Water Isotopes

Water-isotopes mixture contains H_2O, HDO, and D_2O with fractional mass concentrations of C_1, C_2, and C_3, respectively. It was assumed in the previous work (6) that these concentrations were locally at equilibrium at every point in the thermal diffusion columns, i.e.

$$H_2O + D_2O \Leftrightarrow 2HDO \tag{1}$$

with the equilibrium constant defined as

$$K_{eq} = \frac{[HDO]^2}{[H_2O][D_2O]} \approx \frac{C_2^2}{C_1 C_3} \tag{2}$$

Since water-isotopes mixture is a ternary system, thus

$$C_1 + C_2 + C_3 = 1 \tag{3}$$

Accordingly, the concentration of HDO (C_2) can be solved from Eqs. (2) and (3) with the expression in term of the concentration of D_2O (C_3) as

$$C_2 = -\frac{K_{eq}}{2} C_3 + \left\{ C_3 K_{eq} \left[1 - \left(1 - \frac{K_{eq}}{4} \right) C_3 \right] \right\}^{1/2} \tag{4}$$

Since the value of K_{eq} is approximately 4 ($K_{eq} = 3.793$ at 30.5°C (6)), Eq. (4) may be reduced to

$$C_2 = -(K_{eq} C_3/2) + K_{eq}^{1/2} C_3^{1/2} \tag{5}$$

The degree of separation for HDO in a Frazier scheme is defined as the concentration difference between the bottom and top ends at the outlet column, i.e.

$$\Delta_2 = C_{2,B} - C_{2,T} \tag{6}$$

$$= -(K_{eq}/2)(C_{3,B} - C_{3,T}) + K_{eq}^{1/2}(C_{3,B}^{1/2} - C_{3,T}^{1/2}) \tag{7}$$

Further, since ($C_{3,B} - C_{3,F}$) and ($C_{3,F} - C_{3,T}$) are very small, and

$$C_{3,B}^{1/2} - C_{3,F}^{1/2} \approx C_{3,F}^{1/2} - C_{3,T}^{1/2} \tag{8}$$

one has

$$\begin{aligned} C_{3,B}^{1/2} - C_{3,T}^{1/2} &= (C_{3,B} - C_{3,T})/(C_{3,B}^{1/2} + C_{3,T}^{1/2}) \\ &\approx (C_{3,B} - C_{3,T})/(2C_{3,F}^{1/2}) \end{aligned} \tag{9}$$

Thus, Eq. (7) becomes

$$\Delta_2 = -(K_{eq}/2)\Delta_3 + (K_{eq}^{1/2}/2C_{3,F}^{1/2})\Delta_3 \tag{10}$$

where Δ_3 is the degree of separation for heavy water (D_2O), i.e.

$$\Delta_3 = C_{3,B} - C_{3,T} \tag{11}$$

Separation Equation for Heavy Water

The schematic diagram of the Frazier scheme is shown in Fig. 1, which is constructed with N flat-plate thermal-diffusion columns of the same size connected in series. The delivery of the supply σ with the feed concentration is accomplished at the entrance of the upper and lower ends in the first flat-plate thermal-diffusion column with length L, plate spacing 2ω and width B, where both streams have the same direction. Sampling of the product is carried out at the ends opposite to the supply entrance. Rabinovic and Sovorov (9, 10) gave an analytical solution for the separation equation of a binary system as

$$\Delta = C_T - C_B \tag{12}$$

$$= \frac{C(1-C)HL}{K}\left\{1 - \left[\frac{HL/K}{(2H/\sigma) + HL/K}\right]^N\right\} \tag{13}$$

where

$$H = \frac{\alpha\overline{\rho}g\overline{\beta}(2\omega)^3 B(\Delta T)^2}{6!\mu T_m} \tag{14}$$

$$K = \frac{\overline{\rho}g^2\overline{\beta}^2(2\omega)^7 B(\Delta T)^2}{9!\mu^2 D} \tag{15}$$

For the enrichment of heavy water from water-isotopes mixture, Yeh and Yang (6) modified the separation equation with the concentration product of a binary system, C(1 − C), replaced by a pseudo feed concentration product A

of heavy water as

$$A = C_{3,F}\{0.05263 - (0.05263 - 0.0135K_{eq})C_{3,F} - 0.027[C_{3,F}K_{eq}(1 - (1 - 0.25K_{eq})C_{3,F})]^{1/2}\} \quad (16)$$

Accordingly, the separation equation for enrichment of heavy water D_2O from H_2O-HDO-D_2O system in N flat-plate thermal diffusion columns of the Frazier scheme can be obtained by modifying Eq. (13) as

$$\Delta_3 = C_{3,B} - C_{3,T} = \frac{A(-H)L}{K}\left\{1 - \left[\frac{HL/K}{(2H/\sigma) + HL/K}\right]^N\right\} \quad (17)$$

Recovery of Deuterium

The deuterium recovery Δ_D in a Frazier scheme may be defined from the molecular weights of HDO and D_2O as

$$\Delta_D = C_{D,B} - C_{D,T} \quad (18)$$

$$= \left[\frac{2}{19}C_{2,B} + \frac{4}{20}C_{3,B}\right] - \left[\frac{2}{19}C_{2,T} + \frac{4}{20}C_{3,T}\right]$$

$$= \frac{2}{19}\Delta_2 + \frac{4}{20}\Delta_3 \quad (19)$$

Substituting Eqs. (10) and (17) into Eq. (19), we have

$$\Delta_D = \Delta_3\left[0.2 - (K_{eq}/19) + (K_{eq}/C_{3,F})^{1/2}/19\right] \quad (20)$$

$$= \frac{F(-H)L}{K}\left\{1 - \left[\frac{HL/K}{(2H/\sigma) + HL/K}\right]^N\right\} \quad (21)$$

where

$$F = A[0.2 - (K_{eq}/19) + (K_{eq}/C_{3,F})^{1/2}/19] \quad (22)$$

EFFECT OF PLATE ASPECT RATIO ON PERFORMANCE

If we define the plate aspect ratio as

$$\xi = L/B \quad (23)$$

then

$$L = (S\xi)^{1/2} \tag{24}$$

$$B = (S/\xi)^{1/2} \tag{25}$$

where S (=BL) is the plate surface area. If the following constants are also defined from Eqs. (14) and (15) as

$$a = -H/B \tag{26}$$

$$b = K/B \tag{27}$$

Eq. (21) becomes

$$\Delta_D = \frac{Fa(S\xi)^{1/2}}{b}\{1 - [1 + (2b/\sigma\xi)]^{-N}\} \tag{28}$$

Eq. (28) can be rewritten to obtain the expression for calculating the production rate and plate surface area as

$$\sigma = (2b/\xi)\left\{\left[1 - \frac{\Delta_D}{(Fa/b)(S\xi)^{1/2}}\right]^{-1/N} - 1\right\}^{-1} \tag{29}$$

$$S = \frac{(b^2\Delta_D^2/F^2a^2)}{\xi\{1 - [(2b/\sigma\xi) + 1]^{-N}\}^2} \tag{30}$$

Maximum Separation with Plate Surface Area Fixed

With constant production rate and plate surface area S, the optimum plate aspect ratio ξ_Δ for maximum separation $\Delta_{D,\max}$ is obtained by partially differentiating Eq. (28) with respect to ξ and setting $\partial\Delta_D/\partial\xi = 0$. After differentiation and simplification, we have

$$W^{N+1} - (2N + 1)W + 2N = 0 \tag{31}$$

where

$$W = (2b/\sigma\xi_\Delta) + 1 \tag{32}$$

Therefore, the optimum plate aspect ratio for maximum separation is expressed as

$$\xi_\Delta = (2b/\sigma)/(W - 1) \tag{33}$$

in which W is determined from Eq. (31) once column number of the Frazier

scheme is specified. From Eqs. (24) and (25), we also obtain

$$L_\Delta = (S\xi_\sigma)^{1/2} = \sqrt{2}[(bS/\sigma)/(W-1)]^{1/2} \tag{34}$$

$$B_\Delta = (S/\xi_\sigma)^{1/2} = (1/\sqrt{2})[(\sigma S/b)(W-1)]^{1/2} \tag{35}$$

Consequently, the maximum separation may be obtained from Eq. (28) by the substitution of Eq. (33). The result is

$$\Delta_{D,\max} = \left[\frac{(2F^2a^2S/b)}{\sigma}\right]^{1/2}[(1-W^{-N})/(W-1)^{1/2}] \tag{36}$$

Equations (33) and (36) show that whereas $\Delta_{D,\max}$ depends on the thermal diffusion constant α ξ_Δ is independent of α. The problem of finding the maximum separation $\Delta_{D,\max}$ and the best plate aspect ratio ξ_Δ for a specified flow rate σ can readily be solved by using Eqs. (33) and (36) since a, b, and S are constants for a given column and system. This problem, however, is rather artificial and academic in nature and therefore two other more practical problems will be discussed:

(i) finding the maximum production rate and the corresponding best plate aspect ratio for a given column operated in a manner to obtain predetermined degree of separation and plate surface area, and
(ii) finding the minimum plate surface area and the corresponding best plate aspect ratio required to obtain a specific degree of separation and production rate.

Maximum Production Rate with Plate Surface Area Fixed

The optimum plate aspect ratio for maximum production rate with the degree of separation Δ_D and plate surface area S specified, is obtained by partially differentiating Eq. (29) with respect to ξ and setting $\partial\sigma/\partial\xi = 0$. After differentiation and simplification, this gives

$$\xi_\sigma = (b^2\Delta_D^2/F^2a^2S)/(1-W^{-N})^2 \tag{37}$$

Therefore,

$$L_\sigma = (S\xi_\sigma)^{1/2} = (b\Delta_D/Fa)/(1-W^{-N}) \tag{38}$$

$$B_\sigma = (S/\xi_\sigma)^{1/2} = (FaS/b\Delta_D)(1-W^{-N}) \tag{39}$$

Consequently, the maximum production rate may be obtained from Eq. (29) by substitution of Eq. (37). The result is

$$\sigma_{\max} = (2F^2a^2S/b\Delta_D^2)[(1-W^{-N})^2/(W-1)] \tag{40}$$

It is very interesting to show from Eq. (29) that the plate aspect ratio for maximum separation is also the plate aspect ratio required to obtain the maximum production rate $\sigma_{\max}$; for a given scheme which is to give a specified degree of separation Δ_D. Actually, the maximization yields an expression which is identical with Eq. (31) and consequently the solutions for the optimum plate aspect ratio ξ_σ for maximum production rate, Eqs. (37) and (40), are identical to those given by Eqs. (33) and (36) when ξ_Δ and σ are replaced by ξ_σ and $\sigma_{\max}$, respectively, and when $\Delta_{D,\max}$ is replaced by Δ_D.

Minimum Plate Surface Area

The optimum plate aspect ratio for minimum plate surface area with the degree of separation Δ_D and flow rate σ specified, is obtained by partially differentiating Eq. (30) with respect to ξ and setting $\partial S/\partial\xi = 0$. After differentiation and simplification, one obtains

$$\xi_S = (2b/\sigma)/(W-1) \tag{41}$$

Therefore,

$$S_{\min} = \frac{\Delta_D^2 b\sigma}{2F^2a^2}[(W-1)/(1-W^{-N})^2] \tag{42}$$

$$L_S = (S_{\min}\xi_S)^{1/2} = (b\Delta_D/Fa)/(1-W^{-N}) \tag{43}$$

$$B_S = (S_{\min}/\xi_S)^{1/2} = (\Delta_D\sigma/2Fa)[(W-1)/(1-W^{-N})] \tag{44}$$

It is also easy to show from Eq. (30) that the maximization yields an expression which is identical with Eq. (31) and consequently the solutions for the optimum plate aspect ratio ξ_S for minimum plate surface area, Eqs. (41) and (42), are identical to those given by Eqs. (33) and (36) when $\Delta_{D,\max}$ and S are replaced by Δ_D and $S_{\min}$, respectively.

Numerical Example

The improvement in performance resulting from operating at the optimal plate aspect ratio may be illustrated by using the experimental data of the previous work (6). for enrichment of heavy water from the H_2O-HDO-D_2O system: $\Delta T = 47-14 = 33^\circ$C, $T_m = 30.5^\circ$C, $K_{eq} = 3.793$, $2\omega = 0.016$in. $= 0.0406$ cm, $L = 177$ cm, $B = 10$ cm, $H = -1.473\times10^{-4}$g/s $= -0.53$ g/h, $K = 1.597\times10^{-3}$ g $\cdot$ cm/s $= 5.576$ g $\cdot$ cm/h. Some values of A and F were calculated from Eqs. (16) and (22) and are given in Table 1. Actually, the thermal diffusion column employed in previous work was a concentric tube device with a 1.282 in. inside diameter of outer tube and 1.25 in. outside diameter of the

Table 1. Some values of A and F with $K_{eq} = 3.793$ at $T_m = 30.5^\circ C$

$C_{3,F}$	0.1	0.3	0.5	0.7	0.9
$A \times 10^2$	0.359	0.709	0.761	0.591	0.237
$F \times 10^2$	0.1165	0.1329	0.1106	0.0726	0.0257

inner tube, and the annular space (plate spacing) is small (0.032/2 in), which is the essential design of a thermal diffusion column for saving energy consumption since the driving force for thermal diffusion is the temperature gradient ($\Delta T/2w$), and in order to apply not large ΔT, we must arrange the annular space ($2w$) as small as possible. In the meantime, the curvature of this concentric tube with such small annular space can be neglected and this system may be considered as a flat-plate system.

From these numerical values the maximum recovery of deuterium, $\Delta_{D,\max}$, and maximum production rate, $\sigma_{\max}$, as well as their corresponding plate aspect ratios, were calculated from the appropriate equations with the plate surface area, $S = LB$, equal to 1770 cm^2. The results for maximum recovery are presented in Table 2 while those of maximum production rate are given in Table 3. The minimum plate surface area S_{min} and its corresponding optimal plate aspect ratio were also calculated with given recovery Δ_D and production rate σ. The results are presented in Table 4. The improvements in performance by operating at the optimal plate aspect ratios may be illustrated by

$$I_\Delta = [\Delta_{D,\max} - \Delta_D]/\Delta_D \tag{45}$$

$$I_\sigma = [\sigma_{\max} - \sigma]/\sigma \tag{46}$$

$$I_S = [S - S_{\min}]/S_{\min} \tag{47}$$

The results are also presented in Tables 2–4.

RESULTS AND DISCUSSION

It is shown in Table 2 that the optimal plate aspect ratio ξ_Δ for maximum recovery $\Delta_{D,\max}$ increases as the flow rate decreases or when the column number N increases. Improvement in deuterium recovery I_Δ based on the separation obtained at $\xi = 17.7$ is achieved, especially for the case where ξ_Δ goes far from 17.7. However, when $N = 10$ and $\sigma = 0.511$ g/h, or when $N = 20$ and $\sigma = 1.012$ g/h, or when $N = 40$ and $\sigma = 2.016$ g/h, we have $\xi_\Delta = \xi = 17.7$ and $\Delta_{D,\max} = \Delta_D$. This means that the experimental system of previous work (6) operating at these flow rates is exactly the case such that the plate aspect ratios are optimal and the recoveries are maximum.

Table 2. Comparison of separations, $\Delta_{D,\max}$ and Δ_D, obtained at $\xi = \xi_\Delta$ and at $\xi = 17.7$, respectively, with S = 1770 cm^2: (a) N = 10; (b) N = 20; (c) N = 40

		$C_{3,F} = 0.1$		$C_{3,F} = 0.3$		$C_{3,F} = 0.5$		$C_{3,F} = 0.7$		$C_{3,F} = 0.9$		
σ (g/h)	ξ_Δ	Δ_D (%)	$\Delta_{D,\max}$(%)	Δ_D (%)	$\Delta_{D,\max}$(%)	Δ_D(%)	$\Delta_{D,\max}$ (%)	Δ_D(%)	$\Delta_{D,\max}$(%)	Δ_D(%)	$\Delta_{D,\max}$(%)	I_Δ
(a)												
0.1	90.48	1.94	3.04	2.22	3.47	1.85	2.89	1.21	1.89	0.43	0.67	57
0.4	20.67	1.50	1.52	1.72	1.74	1.43	1.45	0.94	0.95	0.33	0.34	1
(0.511)	(17.70)	(1.35)	(1.35)	(1.54)	(1.54)	(1.28)	(1.28)	(0.84)	(0.84)	(0.30)	(0.30)	0
1.6	5.17	0.63	0.76	0.72	0.87	0.60	0.72	0.39	0.47	0.14	0.17	22
6.4	1.29	0.18	0.38	0.21	0.44	0.17	0.36	0.11	0.24	0.04	0.08	109
(b)												
0.1	179.14	1.96	4.37	2.24	4.99	1.86	4.15	1.22	2.73	0.43	0.96	123
0.4	44.79	1.85	2.19	2.12	2.49	1.76	2.08	1.16	1.36	0.41	0.48	18
(1.012)	(17.70)	(1.38)	(1.38)	(1.57)	(1.57)	(1.31)	(1.31)	(0.86)	(0.86)	(0.30)	(0.30)	0
1.6	11.20	1.05	1.09	1.20	1.25	1.00	1.04	0.66	0.68	0.23	0.24	4
6.4	2.80	0.35	0.55	0.40	0.62	0.33	0.52	0.22	0.34	0.08	0.12	57
(c)												
0.1	356.86	1.96	6.23	2.24	7.11	1.86	5.91	1.22	3.88	0.43	1.37	218
0.4	89.22	1.95	3.12	22.23	3.54	1.85	2.96	1.22	1.94	0.43	0.69	59
1.6	22.30	1.54	1.56	1.76	1.78	1.46	1.48	0.96	0.97	0.34	0.34	1
(2.016)	(17.70)	(1.39)	(1.39)	(1.58)	(1.58)	(1.32)	(1.32)	(0.87)	(0.87)	(0.31)	(0.31)	0
6.4	5.58	0.64	0.78	0.72	0.89	0.60	0.74	0.40	0.49	0.14	0.17	22

Table 3. Comparison of production rates, σ_{max} and σ, obtained at $\xi = \xi_\sigma$ and at $\xi = 17.7$, respectively, with S = 1770 cm^2: (a) N = 10; (b) N = 20; (c) N = 40

	Δ_D (%)								
Δ_D/F	$C_{3,F} = 0.1$	$C_{3,F} = 0.3$	$C_{3,F} = 0.5$	$C_{3,F} = 0.7$	$C_{3,F} = 0.9$	σ (g/h)	ξ_σ	σ_{max} (g/h)	I_σ
(a)									
16.69	1.94	2.22	1.85	1.21	0.67	0.1	36.88	0.245	145
12.91	1.50	1.72	1.43	0.94	0.34	0.4	22.07	0.410	3
(11.56)	(1.35)	(1.54)	(1.28)	(0.84)	(0.30)	(0.511)	(17.70)	(0.511)	0
5.38	0.63	0.72	0.60	0.39	0.17	1.6	3.83	2.36	48
1.56	0.18	0.21	0.17	0.11	0.08	6.4	0.32	28.08	339
(b)									
16.80	1.96	2.24	1.86	1.22	0.96	0.1	35.90	0.499	399
15.91	1.85	2.12	1.76	1.16	0.48	0.4	32.20	0.556	39
(11.80)	(1.38)	(1.57)	(1.31)	(0.86)	(0.30)	(1.012)	(17.70)	(1.012)	0
9.04	1.05	1.20	1.00	0.66	0.24	1.6	10.40	1.72	8
2.99	0.35	0.40	0.33	0.22	0.12	6.4	1.14	15.75	146
(c)									
16.81	1.96	2.24	1.86	1.22	1.37	0.1	35.26	1.012	912
16.77	1.95	2.23	1.85	1.22	0.69	0.4	35.09	1.017	154
13.23	1.54	1.76	1.46	0.96	0.34	1.6	21.84	1.634	2
(11.91)	(1.39)	(1.58)	(1.32)	(0.87)	(0.31)	(2.016)	(17.70)	(2.016)	0
5.45	0.64	0.72	0.60	0.40	0.17	6.4	3.71	9.630	50

Table 4. Comparison of plate surface areas, S_{min} and $S = 1770\ cm^2$, required at $\xi = \xi_\Delta$ and at $\xi = 17.7$, respectively, (a) N = 10; (b) N = 20; (c) N = 40

Δ_D/F	σ (g/h)	ξ_S(%)	S_{min} (cm^2)	I_S (%)
(a)			(cm^2)	
16.69	0.1	90.48	722	145
12.91	0.4	20.67	1727	2
(11.56)	(0.511)	(17.70)	1770	0
5.38	1.6	5.17	1110	59
1.56	6.4	1.29	403	339
(b)				
16.80	0.1	179.14	354	400
15.91	0.4	44.79	1273	39
(11.80)	(1.012)	(17.70)	1770	0
9.04	1.6	11.20	1643	8
2.99	6.4	2.80	719	146
(c)				
16.81	0.1	356.86	175	911
16.77	0.4	89.22	696	154
(11.91)	(2.016)	(17.70)	1770	0
5.45	6.4	5.58	1176	51

The optimal plate aspect ratio ξ_σ for maximum production rate σ_{max} increases when the degree of deuterium recovery increases, as shown in Table 3. Improvement in production rate I_σ based on the production rate obtained at $\xi = 17.7$, is achieved, especially for the case where the optimal plate aspect ratio goes far from 17.7. However, when N = 10 and (Δ_D/F) = 11.56, or when N = 20 and (Δ_D/F) = 11.8, or when N = 40 and (Δ_D/F) = 11.91, one has $\xi_\Delta = \xi = 17.7$ and $\sigma_{max} = \sigma$. Therefore, the experimental system of the previous work (6) operating for these specified degrees of recovery is exactly the case such that the plate aspect ratios are optimal and the production rates are maximum.

It is seen in Table 4 that the optimal plate aspect ratio ξ_S for minimum plate surface area S_{min} increases when the degree of recovery Δ_D/F increases and production rate decreases. Improvement in the reduction of plate surface area I_S based on the plate surface area of $1770\ cm^2$ with $\xi = 17.7$ is achieved, especially for the case such that ξ_S goes far from 17.7. However, when N = 10, (Δ_DF) = 11.56 and $\sigma = 0.511$ g/h, or when N = 20, (Δ_D/F) = 11.8 and $\sigma = 1.012$ g/h, or when N = 40, (Δ_D/F) = 11.91 and $\sigma = 2.016$ g/h, we have $\xi_\Delta = \xi = 17.7$ and $S_{min} = S = 1770\ cm^2$. Therefore, the experimental system of the previous work (6) operating at these required conditions is exactly the case such that the plate aspect ratios are optimal and the plate surface areas are minimum.

CONCLUSION

The equations for estimating the optimal plate aspect ratios, as well as the corresponding maximum recovery, maximum production rate, and minimum plate surface area in flat-plate thermal diffusion columns of the Frazier scheme for recovery of deuterium from water-isotopes mixture, have been derived. It was found that all optimal plate aspect ratios for $\Delta_{D,\max}$, $\sigma_{\max}$, and $S_{\min}$ are independent of feed concentration $C_{3,F}$. The improvement in performance was illustrated numerically and the results are presented in Tables 2-4. It is seen from these tables that considerable improvement is obtainable if the operation is carried out with the optimal plate aspect ratio.

The cost of carrying out deuterium recovery from water-isotopes mixture in thermal diffusion columns includes two main contributions, i.e. fixed charges and operating expenses. The fixed charges are roughly proportional to the cost of equipment, primarily the plate surface area S(=BL), while the major contribution to the operating costs is heating. The heat transfer rate is also proportional to the plate surface area (heat transfer area) if $\Delta T/2\omega$ or both ΔT and 2ω are specified. Since the maximum recovery and production rate of deuterium are obtained with a constant plate surface area, the values of ξ_Δ and $\Delta_{D,\max}$ in Table 2, as well as the values of ξ_σ and $\sigma_{\max}$ in Table 3 were calculated with the total cost fixed. On the other hand, the use of a minimum plate surface area will minimize both fixed charges and operating expenses, and therefore the values of $S_{\min}$ and ξ_S in Table 4 provide conditions for minimum total costs with a specified removed rate ($\Delta_D\ \sigma/2$).

NOMENCLATURE

A	constant defined by Eq. (16) with $C_{3,F}$ and K_{eq} as parameters
B	plate width, (cm)
C_i	fractional mass concentration of component i, i = 1,2,3 and D for H_2O, HDO, and D_2O, and D, respectively
$C_{i,B}$, $C_{i,T}$	C_i in the product streams of outlet column existing from the bottom and top ends
C_B, C_T	C in the product streams of outlet column for a binary system
$C_{3,F}$	C_3 in the feed streams of the entrance column
D	ordinary diffusion coefficient, (cm^2/s)
g	gravitational acceleration, (cm/s^2)
H	system constant defined by Eq. (14), (g/s)
I_Δ, I_σ, I_S	improvement in performance defined by Eqs. (45)–(47)
K	system constant defined by Eq. (15), ($g \cdot cm/s$)
K_{eq}	mass-fractional equilibrium constant of H_2O-HDO-D_2O system
L	plate length, (cm)

N	column number of a Frazier scheme
S	BL, plate surface area, (cm^2)
S_{min}	minimum value of S, (cm^2)
T_m	mean absolute temperature, (K)
ΔT	difference in temperature of hot and cold surfaces, (K)

Greek Symbols

α	thermal diffusion constant
β	$-(\partial\rho/\partial T)$ evaluated at T_m, ($g/cm^3 \cdot K$)
Δ	$C_B - C_T$ for a binary system
Δ_i	$C_{i,B} - C_{i,T}$, i = 1,2,3 and D for H_2O, HDO, D_2O, and D, respectively
$\Delta_{D,max}$	maximum value of Δ_D
μ	absolute viscosity, (Pa · s)
ξ	L/B, plat aspect ratio
ξ_Δ, ξ_σ, ξ_S	optimum value of ξ
ρ	mass density, (g/cm^3)
σ	mass flow rate, (g/h)
σ_{max}	maximum value of σ, (g/h)
ω	one half of the plate spacing of the column, (cm)

REFERENCES

1. Iwai, Y., Yamanishi, T., Nakamura, H., Isobe, K., Nishi, M., and Willms, R.S. (2002) Numerical estimation method of the hydrogen isotope inventory in hydrogen isotope separation system for fusion reactor. *J. Nuclear Sci. and Technol.*, 39: 661.
2. Kakiuchic, M. (2001) Fraction of hydrogen isotopes in crystal water of copper Chloride dehydrate-saturated solution-water vapor system. *Geochemical J.* 35: 277.
3. Clusius, K. and Dickel, G. (1938) New process for separation of gas mixtures and isotopes. *Naturwiss.*, 26: 546.
4. Clusius, K. and Dickel, G. (1939) The separation-tube process for liquids. *Naturwiss.*, 27: 148.
5. Furry, W.H., Jones, R.C., and Onsager, L. (1939) On the theory of isotopes separation by thermal diffusion. *Phys. Rev.*, 55: 1083.
6. Yeh, H.M. and Yang, S.C. (1984) The enrichment of heavy water in a batch-type thermal diffusion column. *Chem. Eng. Sci.*, 39: 1277.
7. Kim, J., Park, S.E., Kim, T.S., Jeong, D.Y., and Ko, K.H. (2004) Isotopic water separation using AGMD and VEMD. *Nukleonika*, 49: 137.
8. Frazier, D. (1962) Analysis of transverse flow thermal diffusion. *Ind. Eng. Chem. Process Des.*, 1: 237.
9. Rabinovich, G.D. (1976) Theory of thermal diffusion separation according to the Frazier scheme. *Inzh. Fiz. Zh.*, 31: 514.

10. Sovorov, A.V. and Rabinovich, G.D. (1981) Theory of a thermal diffusion apparatus with transverse flows. *Inzh. Fiz. Zh.*, 41: 231.
11. Powers, J.E. and Wilke, C.R. (1957) Separation of liquid by thermal diffusion. *AIChE J.*, 3: 213.
12. Chueh, P.L. and Yeh, H.M. (1976) Thermal diffusion in a flat-plate column inclined for improved performance. *AIChE J.*, 13: 37.
13. Yeh, H.M. (1995) The optimal plate aspect-ratio for the best performance in flat-plate thermal diffusion column. *J. Chem. Eng. Japan.*, 28: 609.